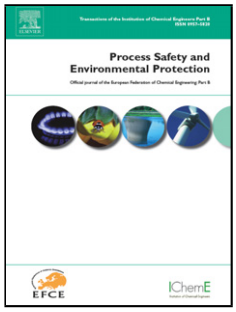

Evaluation of Fe(II)-driven autotrophic denitrification in packed-bed reactors at different nitrate loading rates

Kyriaki Kiskira, Stefano Papirio, Yoan Pechaud, Silvio Matassa, Eric D. van Hullebusch, Giovanni Esposito

PII: S0957-5820(20)31535-4

DOI: https://doi.org/10.1016/j.psep.2020.05.049

Reference: PSEP 2282

To appear in: *Process Safety and Environmental Protection*

Received Date: 23 April 2020

Revised Date: 25 May 2020

Accepted Date: 29 May 2020

Please cite this article as: Kiskira K, Papirio S, Pechaud Y, Matassa S, van Hullebusch ED, Esposito G, Evaluation of Fe(II)-driven autotrophic denitrification in packed-bed reactors at different nitrate loading rates, *Process Safety and Environmental Protection* (2020), doi: https://doi.org/10.1016/j.psep.2020.05.049

Evaluation of Fe(II)-driven autotrophic denitrification in packed-bed reactors at different nitrate loading rates

Kyriaki Kiskira[1,2,*], Stefano Papirio[3], Yoan Pechaud[4], Silvio Matassa[3], Eric D. van Hullebusch[5], Giovanni Esposito[3]

[1]*School of Chemical Engineering, National Technical University of Athens, Heroon Polytechniou 9, 15780, Athens, Greece.*

[2]*Department of Industrial Design and Production Engineering, University of West Attica, Thivon str & P. Rali Ave 250, 12244, Athens, Greece.*

[3]*Department of Civil, Architectural and Environmental Engineering, University of Napoli Federico II, Via Claudio 21, 80125, Napoli, Italy.*

[4]*Laboratoire Géomatériaux et Environnement (LGE), Université Paris-Est, EA 4508, UPEM, 77454, Marne-la-Vallée, France.*

[5] *Institut de Physique du Globe de Paris, CNRS, Université de Paris, F-75005, Paris, France.*

***Corresponding author**

Kyriaki Kiskira

Phone: +30 210 772 3304

Email: kirki.kis@gmail.com

Present address: School of Chemical Engineering, National Technical University of Athens, Heroon Polytechniou 9, 15780, Athens, Greece

Graphical abstract

Highlights

- Fe(II)-driven autotrophic denitrification was investigated in packed-bed reactors
- Higher nitrate loading rates enhanced denitrification performances in PBR1
- The highest specific nitrate removal rate was 14.3 mg NO_3^-/g VS/h
- At constant nitrate loading rate, denitrification efficiency was stable in PBR2
- The *Thiobacillus* enriched mixed culture allowed a long-term process stability

Abstract

Nowadays, nitrate represents one of the major contaminants of the hydrosphere, mainly affecting the quality of groundwater intended to the production of drinking water. This study proposes the use of Fe(II)-driven autotrophic denitrification as a high-potential, innovative bioprocess to couple microbially-catalyzed nitrate reduction to Fe(II) oxidation. Two identical up-flow packed bed reactors (PBRs), i.e. PBR1 and PBR2, with granular activated carbon as biofilm carrier were seeded with a *Thiobacillus*-mixed culture and operated for 153 d at different feed nitrate concentrations and hydraulic retention times (HRTs). The results show enhanced nitrate removal rates and efficiencies at increasing nitrate loading rates. In particular, nitrate removal and Fe(II) oxidation up to 85 and 95%, respectively, were achieved in PBR1 at nitrate loading rates as high as 12.5 mg NO_3^-/L/h. Besides not undermining the denitrification efficiency, increasing the nitrate loading rate from 8.1 to 12.5 mg NO_3^-/L/h triggered the specific nitrate removal rates as high as 14.3 mg NO_3^-/g VS/h. In PBR2, Fe(II)-driven denitrification was investigated at a constant nitrate loading rate by concomitantly decreasing the feed nitrate concentration and HRT. Despite the less severe operational conditions, the use of lower nitrate loading rates resulted in a lower nitrate removal efficiency than that obtained in PBR1.

Keywords: Nitrate, autotrophic denitrification, ferrous iron, loading rate, packed-bed reactor

1. Introduction

Due to the steep growth of human population, a rampant industrialization and intensive agricultural practices, nitrate (NO_3^-) contamination of freshwater reservoirs is becoming a serious global concern, with significant impacts on the environment and on human health (Su et al., 2018b; Liu et al., 2018a). Nitrate pollution is mainly due to the runoff of nitrogen-containing fertilizers and the discharge of improperly treated industrial and domestic wastewaters (Chen et al., 2014; Han et al., 2018). In particular, mining activities are heavily responsible of nitrate release due to the extensive use of ammonium nitrate fuel oil (ANFO) explosives, which contaminates process water together with several heavy metal species, including iron in the form of Fe(II) (Papirio et al., 2014). In view of safeguarding potable water resources and their organoleptic characteristics, the World Health Organization (WHO) has set limits for nitrate in drinking water at 50 mg NO_3^-/L (WHO, 2004).

Physicochemical and biological processes are the leading technologies for the removal of nitrate from water (Huno et al., 2018). Conventional physicochemical methods are ion exchange, reverse osmosis, adsorption and electrodialysis (Hu et al., 2019; Huang et al., 2020). However, the high costs of these processes and the stringent discharge limits on nutrients have boosted the development and success of modern biotechnologies (Liu et al., 2018b; Kostrytsia et al., 2018; Wang et al., 2020b). Among these, heterotrophic denitrification is a well-established process, which has reached a wide diffusion owing to its high efficiency and small amount of hazardous by-products formation (Zou et al., 2014; 2015). However, heterotrophic denitrifying bacteria require a carbon source, making this process not suitable for the treatment of waters characterized by a low C/N ratio (Deng et al., 2020). Indeed, the addition of external carbon would result in extra operating costs as well as in the presence of organic residues generating secondary pollution (Bi et al., 2019; Zhang et al., 2019).

As an alternative biotechnology to heterotrophic denitrification, Fe(II)-driven autotrophic denitrification allows to simultaneously remove nitrate and recover iron through the formation of Fe(III) precipitates (Kiskira et al., 2017a). The first microorganisms capable of performing biological nitrate-dependent Fe(II) oxidation were discovered approximately 25 years ago (Straub et al., 1996). Since then, many other microbial species responsible for Fe(II)-driven denitrification have been observed and their optimal growth conditions have been extensively

reviewed (Kiskira et al., 2017a). Fe(II)-based denitrification has proven particularly effective even in the presence of heavy metals (Kiskira et al., 2018) due to the co-precipitation and adsorption of metals on the Fe(III) biominerals produced by anaerobic Fe(II)-oxidizing denitrifiers (Bryce et al., 2018; Kiskira et al., 2019; Wang et al., 2019). However, only limited research efforts have thus far been done to evaluate the potential of the process in continuous flow bioreactors, which are the most widely used setups in real-scale applications.

The use of up-flow anaerobic sludge bed (UASB) reactors has been investigated at different operating conditions, such as decreasing hydraulic retention times (HRTs) and pH (Zhang et al., 2015, 2018). Nitrate removal as high as 90 and 98% in UASB reactors were obtained by Wang et al. (2017) and Wang et al. (2020a), respectively. Despite the high efficiency observed, the main limitation of UASB systems seems to be the occurrence of iron encrustation around the microbial cells, hindering the long-term performance of the reactors (Zhang et al., 2015, 2018; Wang et al., 2017). Analogously, immobilized cell systems such as up-flow biofilters and moving bed biological reactors (MBBRs) showed a high nitrate removal (i.e. > 90%) at HRTs lower than 24 h (Zhou et al., 2016; Su et al., 2018a). Nonetheless, the high energy required to overcome the head losses and clogging in biofilters and maintain the biofilm carriers in suspension in MBBRs represent the main drawbacks of such systems.

In this context, up-flow packed bed reactors (PBRs) have proven very effective for denitrification of industrial wastewater (Huno et al., 2018), while being extremely simple, easy to maintain and cost-effective systems (Di Capua et al., 2015). A biofilm of denitrifiers grows around a carrier material that is made up of particles with a high specific surface area such as polymeric pellets and activated carbon (Di Capua et al., 2015). The biofilm formation can be stimulated by high feed nitrate and Fe(II) concentrations, with the latter being possible when chelating agents (e.g. EDTA) are used (Zhou et al., 2016). In this work, biological nitrate removal through Fe(II)-driven autotrophic denitrification in the presence of EDTA was investigated in two identical up-flow 1 L PBRs fed with different influent nitrate concentrations and operated for a period of 153 days. In view of achieving long-

term process stability and efficiency under continuous flow settings, the bioreactors were seeded with an acclimated *Thiobacillus*-mixed culture, and parameters such as HRT and nitrate loading rate were varied to evaluate their influence on nitrate removal and Fe(II) oxidation.

2. Material and methods

2.1 Reactor design

Two identical up-flow PBRs were used to investigate Fe(II)-mediated autotrophic denitrification in continuous flow experiments. Figure 1 shows the schematic of the reactors. Both PBRs were made of Plexiglas, with height and internal diameter being 24 and 8 cm, respectively, corresponding to a working volume of 0.98 L. The bed had a height of 16 cm and consisted of Filtrasorb®200 granular activated carbon (Calgon Carbon, USA), with diameter in the range 0.4-1.7 mm (Papirio et al., 2014), which was used as biomass carrier. Glass pearls with a diameter in the range 0.4-1.0 cm were placed at the bottom of the reactors to sustain activated carbon and avoid the clogging of the inlet tap. The effluent was discharged by gravity from an outlet port located 3.5 cm above the top of the filling material. A port located in the effluent line was used for sampling.

Figure 1: Schematic of the up-flow packed bed reactors used for Fe(II)-driven denitrification.

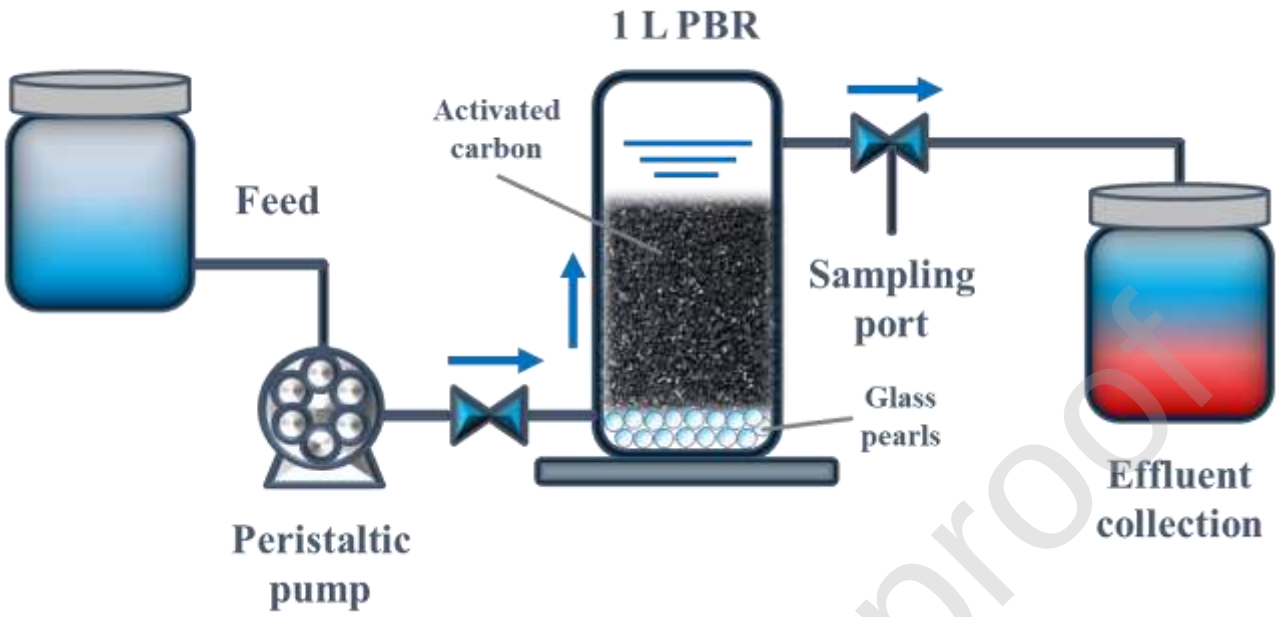

2.2 Inoculum and reactor start-up

A *Thiobacillus*-dominated mixed culture, previously enriched on both thiosulfate and Fe(II) as electron donors (Kiskira et al., 2017b), was inoculated in the two reactors. The PBRs were seeded with 50 mL of the microbial culture, having an initial volatile suspended solid (VSS) concentration of approximately 200 mg VSS/L. After seeding, the bioreactors were flushed with nitrogen gas to establish anoxic conditions. Both reactors were first operated under batch conditions for 1 week in order to guarantee a sufficient acclimation phase. The feed Fe(II) and NO_3^- concentrations were 600 and 120 mg/L, respectively. The Fe(II)- and NO_3^--containing salts as well as the mineral medium used are reported by Kiskira et al. (2017b).

2.3 Feed synthetic wastewater and PBR operation

After the acclimation phase, a synthetic wastewater was continuously fed from the bottom of both reactors by means of a 205S/CA manual control peristaltic pump (Watson-Marlow, USA). Initially, the two PBRs (PBR1

and PBR2) were fed with 120 and 60 mg NO_3^-/L and 600 and 300 mg Fe(II)/L, respectively, in order to maintain a Fe(II):NO_3^- ratio of 5:1. As chelator, EDTA was continuously supplemented at an EDTA:Fe(II) molar ratio of 0.5:1, which was optimal to maintain Fe(II) in solution and avoid the inhibition of the denitrifying activity (Kiskira et al., 2017b). The feed solution contained the same minerals and trace elements used in the acclimation phase. The feed pH and temperature were 7.7 and 22±2°C, respectively.

The continuous flow operation of both PBRs was divided into 5 experimental periods (Table 1) along 153 days. The feed nitrate concentration was increased to 250 and 180 mg NO_3^-/L for PBR1 and PBR2, respectively, on day 64. On day 76, 10 mg VSS of the same enriched *Thiobacillus*-mixed culture used as initial inoculum was seeded to stimulate nitrate removal that dropped in PBR1. HRT was gradually decreased from 31 to 20 h for both PBRs from day 93 until the end of operation. On day 116, the operation of the two PBRs was differentiated. In PBR1, the nitrate concentration was maintained stable at 250 mg NO_3^-/L, in order to evaluate the effect of higher nitrate loading rates at decreasing HRTs. Conversely, the nitrate loading rate remained stable at 8.9 mg NO_3^-/L/h in PBR2 (Table 1) by gradually decreasing the influent nitrate concentration from 250 to 180 mg NO_3^-/L according to the HRT used. The process was monitored by sampling both the liquid phase and the attached biomass.

Table 1: Experimental operating periods and conditions used to investigate the effect of nitrate loading rate and hydraulic retention time (HRT) on Fe(II)-driven autotrophic denitrification in two packed-bed reactors (PBRs).

	Time [d]	HRT [h]	Influent nitrate concentration [mg NO_3^-/L]		Nitrate loading rate [mg NO_3^-/L/h]	
			PBR1	**PBR2**	**PBR1**	**PBR2**
Period I	**0-63**	31	120	60	3.9	1.9
Period II	**64-92**	31	250	180	8.1	5.8

Period III	**93-115**	28	250	180 (days 93-107) 250 (days 108-115)	8.9	6.4-8.9
Period IV	**116-139**	24	250	215	10.4	8.9
Period V	**140-153**	20	250	180	12.5	8.9

2.4 Analytical methods

Ferrous iron, nitrate and pH were analyzed every 48 h. The NO_3^- concentration was analyzed by ion chromatography (IC) with chemically suppressed conductivity using an 883 Basic IC Plus system equipped with a Metrosep A Supp 5-150/4.0 column and an 863 Compact IC Autosampler (Metrohm, Switzerland). The liquid samples were filtered with 0.22 μm syringe cellulose membranes (EMD Millipore, USA) prior to IC analysis. Fe(II) was quantified photometrically by using a UV-1800 240V spectrophotometer (Shimadzu, Japan), following the analytical method reported by Ahoranta et al. (2016). Fe(II) determination was performed immediately after sampling to avoid Fe(II) chemical oxidation. The volatile solids (VS) attached to the activated carbon particles were analyzed according to the standard methods (APHA, 1992).

3. Results

Nitrate and Fe(II) evolution was monitored in the continuous flow PBR1 (Fig. 2) and PBR2 (Fig. 3) for 153 days under different operational conditions. Table 2 reports nitrate removal and Fe(II) oxidation efficiencies and specific rates (per gram of VS) at the end of each experimental period in both PBRs.

During period 1 (0-63 days), nitrate removal (Fig. 2B) and Fe(II) oxidation (Fig. 2C) efficiencies reached up to 70 and 85%, respectively, with a specific nitrate removal rate of 8.8 mg NO_3^-/g VS/h in PBR1 (Table 2). The effluent nitrate concentration gradually decreased from 120 to 35 mg NO_3^-/L (Fig. 2B). Fe(II) oxidation

occurred with a Fe(II):NO_3^- ratio in the range 4.7-7.4. In the same period, Fe(II)-mediated denitrification resulted in a decreasing effluent nitrate concentration from 60 till 36 mg NO_3^-/L in PBR2, corresponding to a nitrate removal efficiency of 40% (Fig. 3B).

Table 2: Nitrate removal and Fe(II) oxidation efficiencies (%) and specific rates (mg/g VS/h) obtained at the end of each experimental period in PBR1 and PBR2 along the 153 days of operation.

	Time [d]	Nitrate removal [%]		Fe(II) oxidation [%]		Specific nitrate removal rate [mg NO_3^-/g VS/h]		Specific Fe(II) oxidation rate [mg Fe(II)/g VS/h]		Attached biomass [g VS/L]	
		PBR1	**PBR2**	**PBR1**	**PBR2**	**PBR1**	**PBR2**	**PBR1**	**PBR2**	**PBR1**	**PBR2**
Period I	**0-63**	70	40	85	69	8.8	3.4	52.0	27.6	0.20	0.20
Period II	**64-92**	88	80	93	94	13.3	13.2	68.1	71.2	0.31	0.24
Period III	**93-115**	87	70	94	74	14.2	13.0	66.9	66.6	0.53	0.35
Period IV	**116-139**	87	69	95	72	14.3	12.2	59.0	58.2	0.54	0.40
Period V	**140-153**	85	67	95	69	14.0	11.3	58.9	56.7	0.62	0.50

During the operation of the PBRs in period II (64-92 d), the influent nitrate concentration was doubled to 250 mg NO_3^-/L in PBR1 (Fig. 2B) and increased by 3 times up to 180 mg NO_3^-/L in PBR2 (Fig. 3B). As a result, nitrate removal decreased from 70 to 62% in PBR1 on day 65 (Fig. 2B), immediately after the variation of the operating condition. In contrast, Fe(II)-driven denitrification was enhanced in PBR2. Nitrate removal abruptly increased to 64% (Fig. 3B) on day 64 and Fe(II) oxidation reached 72% (Fig. 3C). At the end of period II (day 92), nitrate removal and Fe(II) oxidation efficiencies further increased to 80 and 94%, respectively, in PBR2. In order to stimulate denitrification in PBR1, 10 mg VSS of enriched biomass was inoculated on day 76. The effluent nitrate concentration gradually decreased, and nitrate removal reached 88% on day 92 (Fig. 2B). Fe(II) oxidation

was enhanced up to 93% (Fig. 2C). At the end of period II, the specific nitrate removal rate in PBR1 was 13.3 mg NO_3^-/g VS/h, matching that of PBR2 that was 13.2 mg NO_3^-/g VS/h (Table 2).

Starting from period III (93-115 d), HRT was gradually decreased in both PBRs (Fig. 2A, 3A) with the aim to evaluate the effect of HRT on the denitrification efficiency. When decreasing HRT from 31 to 28 h and, thus, increasing nitrate loading rate from 8.1 to 8.9 mg NO_3^-/L/h, nitrate removal only decreased by 3% in PBR1 on day 94 (Fig. 2B). From that point until the end of period III, nitrate removal slightly increased and reached 88%, as at the end of period II. The specific nitrate removal rate was 14.2 mg NO_3^-/g VS/h (Table 2). During periods IV (116-139 days) and V (140-153 days), the performance of Fe(II)-mediated denitrification was constant, with nitrate removal and Fe(II) oxidation stably at 86 and 96% (Fig. 2B, 2C), respectively, till the end of PBR1 operation. Denitrification was not affected when decreasing the HRT from 28 to 24 h during period IV and from 24 to 20 h during period V, corresponding to a nitrate loading rate increase from 8.9 to 12.5 mg NO_3^-/L/h. The specific nitrate removal rate reached up to 14.0 mg NO_3^-/g VS/h in PBR1 at the end of the bioreactor operation (Table 2).

At the half of period III (day 108), the influent nitrate concentration was increased from 180 to 250 mg NO_3^-/L in PBR2, setting a nitrate loading rate of 8.9 mg NO_3^-/L/h. Nitrate removal and Fe(II) oxidation, however, constantly decreased and were 10 and 34% lower on day 115 (i.e. end of period III) than those observed on day 92 (Fig. 3B, 3C). In Period IV and V, the HRT and the feed nitrate concentration were simultaneously decreased in order to maintain a stable nitrate loading rate of 8.9 mg NO_3^-/L/h in PBR2 (Table 1, Fig. 3A). A steady state denitrification was observed during days 116-153 with nitrate removal (Fig. 3B) and Fe(II) oxidation (Fig. 3C) of 66 and 70%, respectively. The specific nitrate removal rate decreased to 11.3 mg NO_3^-/g VS/h (Table 2).

Throughout the operation of both PBRs, no nitrite was detected as intermediate of Fe(II)-mediated denitrification and the effluent pH constantly remained in the range 6.4-7.2.

Figure 2: The performance of PBR 1. A) Variation of nitrate loading rate and hydraulic retention time (HRT), and evolution of effluent pH, B) Influent and effluent nitrate concentration and nitrate removal efficiency, C) Influent and effluent Fe(II) concentration and Fe(II) oxidation efficiency.

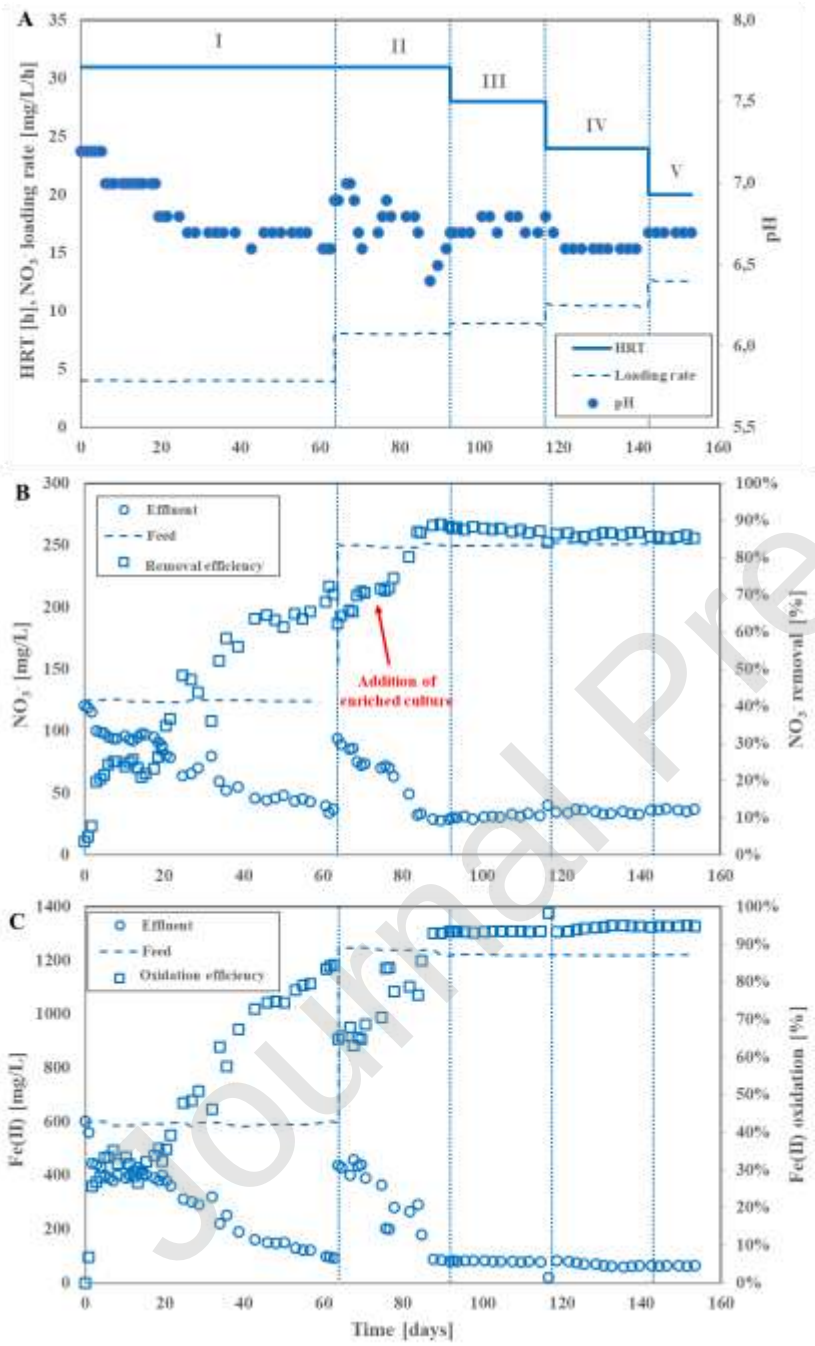

Figure 3: The performance of PBR 2. A) Variation of nitrate loading rate and hydraulic retention time (HRT), and evolution of effluent pH, B) Influent and effluent nitrate concentration and nitrate removal efficiency, C) Influent and effluent Fe(II) concentration and Fe(II) oxidation efficiency.

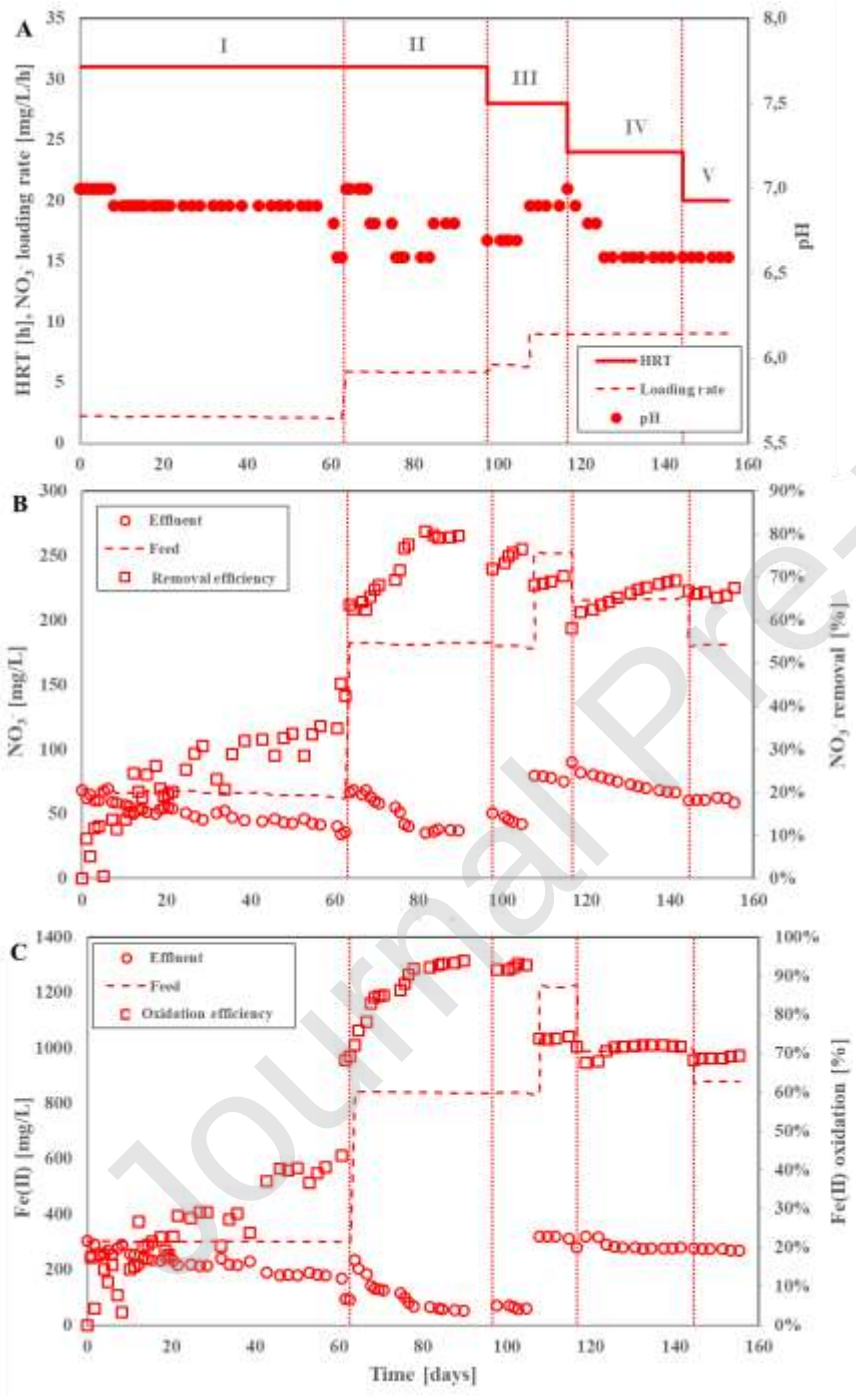

4. Discussion

4.1 Effect of nitrate loading rate on Fe(II)-driven autotrophic denitrification

In this study, the potential of Fe(II)-driven autotrophic denitrification was investigated at varying nitrate loading rates and feed concentrations by using two different feeding strategies in continuous flow PBRs. In PBR1, the feed nitrate concentration was maintained at 250 mg NO_3^-/L from period II onwards while decreasing the HRT from 31 to 20 h, resulting in a nitrate loading rate increasing from 8.1 to 12.5 mg NO_3^-/L/h (Table 1). In PBR2, the feed nitrate concentration and HRT were accordingly decreased from period III onwards in order to ensure a constant nitrate loading rate of 8.9 mg NO_3^-/L/h. The higher nitrate loading rates used during PBR1 operation led to higher nitrate removal efficiencies and specific rates, i.e. respectively up to 88% and 14.3 mg NO_3^-/g VS/h (Table 2). Generally, the specific nitrate removal rates in both PBRs increased as the influent nitrate concentration was risen from 60 to 250 mg NO_3^-/L (Fig. 4) and nitrate removal efficiencies were stable with a stable nitrate loading rate.

In agreement with our study, when the nitrate loading rate increased from 0.8 to 4.2 mg NO_3^-/L/h, the volumetric nitrate removal rate was increased by 20% and reached 4.1 mg NO_3^-/L/h in an MBBR inoculated with a pure culture of *Pseudomonas* sp. SZF15 strain (Su et al., 2018a). Similarly, the nitrate removal rate increased from 0.8 to 1.8 mg NO_3^-/L/h when the nitrate loading rate was increased from 1.3 to 4.2 mg NO_3^-/L/h in a continuous up-flow biofilter packed with sponge iron and seeded with a pure culture of *Microbacterium* sp. W5 (Zhou et al., 2016). Nonetheless, Zhou et al. (2016) observed a 10% decrease of nitrate removal already when the loading rate was increased from 2.9 to 4.2 mg NO_3^-/L/h, and Su et al. (2018a) only investigated nitrate loading rate up to 4.2 mg NO_3^-/L/h. A similar trend was also observed in other studies. When the nitrate loading rate was increased to more than 12.5 mg NO_3^-/L/h (i.e. similar to that used in our study), the volumetric nitrate removal rates dropped by 67% in a UASB reactor operated with an activated sludge culture (Wang et al., 2017). A similar threshold of approximately 12.9 mg NO_3^-/L/h of nitrate loading rate was observed in UASB reactors inoculated

with activated sludge and anaerobic granular sludge cultures, leading to a volumetric nitrate removal rate drop from 5.0 to 3.3 mg NO_3^-/L/h and from 8.3 to 6.6 mg NO_3^-/L/h, respectively (Zhang et al., 2018). When increasing the nitrate loading rate from 7.5 to 10.8 mg NO_3^-/L/h, Zhang et al. (2015) observed an almost 70% lower nitrate removal efficiency and a nitrate removal rate decreasing from 7.9 to 3.0 mg NO_3^-/L/h in a UASB system seeded with an anaerobic granular sludge.

Figure 4: Relationship between the specific nitrate removal rates (per gram of volatile solids) and the feed nitrate concentration in both PBRs.

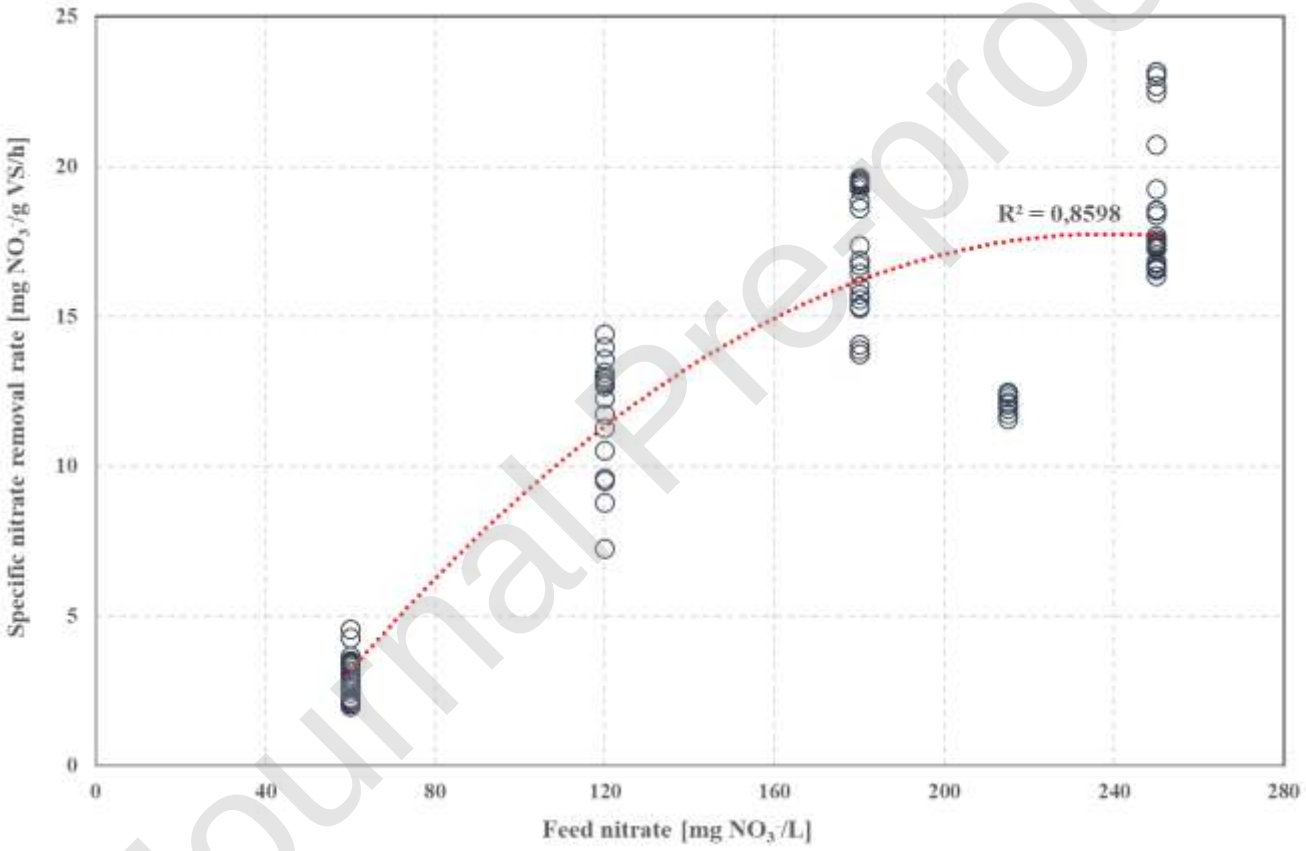

The reason for the discrepancy between the results achieved in our study and those reported in the scientific literature might be due to the longer enrichment on Fe(II) of the *Thiobacillus*-mixed culture, occurred in previous experiments (Kiskira et al., 2017b). Furthermore, the initial 7 d batch-mode incubation phase in the presence of 120 mg NO_3^-/L of feed nitrate likely allowed the acclimation of the denitrifying microorganisms and

an effective colonization of the activated carbon particles. This is also demonstrated by the increasing biomass concentration observed along the operation of both PBRs (Table 2), which indicates the growth of a well-performing biofilm, capable of tolerating higher feed nitrate concentrations and loading rates (Fig. 2B). Rather, the process showed a sudden drop in denitrification performances in concomitance with the decrease in feed nitrate concentrations operated at the beginning of period IV and V, with the nitrate removal efficiency almost entirely recovering during time after each HRT decrease (Fig. 3B).

4.2 The presence of EDTA in the feed and influence of the Fe(II)/NO_3^- ratio

Another possible reason for the higher Fe(II)-driven denitrification performance at the highest nitrate loading rates and influent nitrate concentration was likely due to the supplementation of EDTA with a molar EDTA:Fe(II) ratio of 0.5:1. EDTA chelates Fe(II) and minimizes chemical Fe(II) oxidation with residual oxygen (Chakraborty and Picardal, 2013; Peng et al., 2018). Moreover, EDTA prevents cell encrustation by the biogenic Fe(III) hydroxide minerals, allowing a prolonged activity of microbes (Shelobolina et al., 2003; Chakraborty et al., 2011). The occurrence of cell encrustation probably led to the decrease of nitrate removal efficiency in the studies of Wang et al. (2017) and Zhang et al. (2018), who did not supplement EDTA in the feed. Also, Zhou et al. (2016) observed a recovery of nitrate removal to 90% when starting to add 10 g/L of EDTA to a feed solution containing ferrous iron up to 1800 mg Fe(II)/L, due to a combined lower Fe(II) toxicity and cell encrustation effect. The use of short HRTs (i.e. 8 h) has been reported to hinder cell encrustation by washing out the Fe(III) products, despite the use of a ferrous iron concentration of 800 mg Fe(II)/L and the absence of EDTA in the feed (Tian et al., 2020).

The Fe(II)/NO_3^- ratio is another essential parameter to control in order to obtain a complete denitrification. At the beginning, Fe(II) oxidation occurred with a Fe(II):NO_3^- ratio in the range 4.7-7.4, indicating that part of Fe(II) was most likely oxidized due to the chemical reaction with the residual dissolved oxygen (DO). During the PBR operation, the average ratio between the consumed Fe(II) and nitrate was 5.4 and 4.4 in PBR1 and PBR2

(Fig. 2B,C, 3B,C), respectively, which is in agreement with the theoretical stoichiometry (Sorensen, 1987; Tian et al., 2020) and previous works on the same enriched *Thiobacillus*-mixed culture (Kiskira et al., 2017b; 2018). Other studies on Fe(II)-mediated denitrification in continuous flow systems showed a lower Fe(II)/NO_3^- ratio, i.e. in the range 2.0-2.9 (Zhang et al., 2015; Su et al., 2018a; Zhang et al., 2018) and 3.0-4.0 (Wang et al., 2017; Wang et al., 2020a). A lower Fe(II)/NO_3^- ratio than 4.0 normally indicates a lower nitrogen conversion performance and the production of intermediates such as nitrite and nitrous oxide (Li et al., 2014). This might be the reason of the absence of nitrite throughout the entire operation of both PBRs in our study. Finally, Wang et al. (2017) correlated a fast rise of the Fe(II)/NO_3^- ratio to a reactor failure. A rapid variation of the Fe(II)/NO_3^- ratio was not observed in our study, demonstrating the robustness of the process and the resilience of the biofilm developed.

4.3 Effect of HRT and effluent pH

In this study, the HRT was stepwise decreased from 31 to 28, 24 and 20 h in order to evaluate the adaptation of the *Thiobacillus*-colonized biofilm under more kinetically limiting conditions at increasing (PBR1) or stable (PBR2) nitrate loading rates. Denitrification was not significantly affected in PBR1 when decreasing the HRT, with the nitrate removal efficiency remaining constant at approximately 87% (Table 2, Fig. 2B). This indicates that the denitrifying microorganisms quickly acclimatized to the HRT variations. PBR2 also showed to tolerate the gradual HRT decrease in the presence of a constant nitrate loading rate, but the denitrifiers required a longer acclimation time to remove nitrate with the same efficiency obtained in the previous operating period (Fig. 3B). Globally, the nitrate removal efficiency slightly decreased from 70 to 67% when decreasing the HRT from 28 to 20 h in PBR2 (Table 2), but this was more likely due to the concomitant decrease of the feed nitrate concentration and the constant nitrate loading rate, which stimulated denitrification at a lower extent (see section 4.1).

In contrast with the results here achieved, a little HRT reduction from 18 to 17 h resulted in a decreased performance in terms of both nitrate removal and Fe(II) oxidation from 95 to 60% and from 95 to 38%,

respectively, in an UASB reactor (Zhang et al., 2015). Stable HRTs of 12 and 16 h were used by Zhang et al. (2018) and Wang et al. (2017) in UASB reactors, allowing to obtain nitrate removal efficiencies of 96 and 95%, respectively. A notably high nitrate removal efficiency reported at HRTs of 8.0 (Tian et al., 2020) and 4.4 h (Wang et al., 2020a) was ascribed to the successful washout of the Fe(III) minerals, which otherwise caused cell encrustation and reduced microbial activity. Nonetheless, further investigation on possible shorter HRTs is needed to explore the industrial-scale application of Fe(II)-driven autotrophic denitrification.

With regard to pH, the feed pH was maintained at 7.7 during the entire operation of both PBRs, as Fe(II)-mediated autotrophic denitrification produces acidity and a feed pH higher than 7.0 is recommended (Zhang et al., 2015). Furthermore, a neutral pH environment is necessary to avoid chemical Fe(II)-EDTA oxidation and, thus, stimulate autotrophic denitrification. Indeed, Fe(II) is not favored to act as an electron donor and yield energy in acidic environments, since the redox potential of the ferrous/ferric couple in acidic liquors is approximately +770 mV, i.e. much higher than the +430 mV of the NO_3^-/NO_2^- couple (Schaedler et al., 2018). During denitrification, the effluent pH gradually decreased to 6.4 in both the reactors without significantly affecting the process (Fig. 2A, 3A). In agreement, other studies indicate that nitrate removal was higher than 95% as long as the effluent pH was above 6.0, while a decrease of pH down to 3.0 negatively affected nitrate removal by 80% (Zhang et al., 2015).

5. Conclusions

Fe(II)-mediated autotrophic denitrification in continuous flow PBRs resulted in a nitrate removal percentage higher than 65% and a Fe(II) oxidation of more than 70% along the 153 days of operation. Increasing nitrate loading rates allowed to obtain a higher nitrate removal efficiency, reaching up to 88 and 81% in PBR1 and PBR2, respectively. The biofilm developed onto the granular activated carbon in PBR1 tolerated the stepwise increase of the nitrate loading rate, as demonstrated by the stable nitrate removal efficiencies observed along the HRT decrease from 31 to 20 h at 250 mg NO_3^-/L of feed nitrate. Denitrification displayed a sudden but recoverable loss of performance when lower feed nitrate and HRT were applied in PBR2. The results obtained in this study

are encouraging, especially in terms of the long-term process stability demonstrated by the *Thiobacillus* enriched mixed culture. The coupling of such mixed culture to the easy-to-operate and reliable PBR configuration showed an appealing resilience towards varying process conditions, which stimulates further research efforts in the field of Fe(II)-mediated autotrophic denitrification. Future developments should aim at enabling the process at even lower HRT values in order to pave the way towards the upscaling of this promising nitrate removal biotechnology.

Declaration of interests

The authors declare that they have no known competing financial interests or personal relationships that could have appeared to influence the work reported in this paper.

Acknowledgments

The study was carried out in the framework of the Erasmus Mundus Joint Doctorate ETeCoS^3 (Environmental Technologies for Contaminated Solids, Soils, and Sediments) funded by the European Commission under the grant agreement FPA n°2010-0009. Kyriaki Kiskira was supported by a grant from the Italian Ministry of Education, University and Research (MIUR).

References

1. Ahoranta, S. H., Kokko, M. E., Papirio, S., Özkaya, B. and Puhakka, J. A., (2016). Arsenic removal from acidic solutions with biogenic ferric precipitates, *Journal of Hazardous Materials*, 306, pp. 124-132.

2. American Public Health Association (APHA), (1992). Standard methods for the examination of water and waste water, 18th ed. APHA, AWWA, WPCF.
3. Bi, Z., Zhang, W., Song, G. and Huang, Y., (2019). Iron-dependent nitrate reduction by anammox consortia in continuous-flow reactors: A novel prospective scheme for autotrophic nitrogen removal, *Science of The Total Environment*, 692, pp. 582-588.
4. Bryce, C., Blackwell, N., Schmidt, C., Otte, J., Huang, Y.M., Kleindienst, S., Tomaszewski, E., Schad, M., Warter, V., Peng, C. and Byrne, J.M., (2018). Microbial anaerobic Fe (II) oxidation–Ecology, mechanisms and environmental implications, *Environmental Microbiology*, 20, pp. 3462-3483.
5. Chakraborty, A., Roden, E.E., Schieber, J. and Picardal, F., (2011). Enhanced growth of *Acidovorax* sp. strain 2AN during nitrate-dependent Fe (II) oxidation in batch and continuous-flow systems, *Applied and Environmental Microbiology*, 77, pp. 8548-8556.
6. Chakraborty, A. and Picardal, F., (2013). Induction of Nitrate-Dependent Fe(II) Oxidation by Fe(II) in *Dechloromonas* sp. Strain UWNR4 and *Acidovorax* sp. Strain 2AN, *Applied and Environmental Microbiology*, 79, pp. 748-752.
7. Chen, C., Liu, L.H., Lee, D.J., Guo, W.Q., Wang, A.J., Xu, X.J., Zhou, X., Wu, D.H., Ren and N.Q., (2014). Integrated simultaneous desulfurization and denitrification (ISDD) process at various COD/sulfate ratios, *Bioresource Technology*, 155, pp. 161-169.
8. Deng, S., Peng, S., Xie, B., Yang, X., Sun, S., Yao, H. and Li, D., (2020). Influence Characteristics and Mechanism of Organic Carbon on Denitrification, N2O Emission and NO_2^- Accumulation in the Iron [Fe (0)]-oxidizing Supported Autotrophic Denitrification Process, *Chemical Engineering Journal*, pp. 124736-124748.
9. Di Capua, F., Papirio, S., Lens, P.N. and Esposito, G., (2015). Chemolithotrophic denitrification in biofilm reactors, *Chemical Engineering Journal*, 280, pp. 643-657.

10. Han, J., Shi, L., Wang, Y., Chen, Z. and Xu, J., (2018). Investigation of ferrous iron-involved anaerobic denitrification in three subtropical soils of southern China, *Journal of Soils and Sediments*, 18, pp. 1873-1883.
11. Hu, Z., Li, D., Deng, S., Liu, Y., Ma, C. and Zhang, C., (2019). Combination with catalyzed Fe (0)-carbon microelectrolysis and activated carbon adsorption for advanced reclaimed water treatment: simultaneous nitrate and biorefractory organics removal, *Environmental Science and Pollution Research*, 26, pp. 5693-5703.
12. Huang, W., Gong, B., Wang, Y., Lin, Z., He, L., Zhou, J. and He, Q., (2020). Metagenomic analysis reveals enhanced nutrients removal from low C/N municipal wastewater in a pilot-scale modified AAO system coupling electrolysis, *Water Research*, 173, pp. 115530-115541.
13. Huno, S.K., Rene, E.R., van Hullebusch, E.D. and Annachhatre, A.P., (2018). Nitrate removal from groundwater: a review of natural and engineered processes, *Journal of Water Supply: Research and Technology-Aqua*, 67, pp. 885-902.
14. Kiskira, K., Papirio, S., van Hullebusch, E. D. and Esposito, G. (2017a). Fe(II)-mediated autotrophic denitrification: A new bioprocess for iron bioprecipitation/biorecovery and simultaneous treatment of nitrate-containing wastewaters, *International Biodeterioration & Biodegradation*, 119, pp. 631-648.
15. Kiskira, K., Papirio, S., van Hullebusch, E.D. and Esposito, G., (2017b). Influence of pH, EDTA/Fe (II) ratio, and microbial culture on Fe (II)-mediated autotrophic denitrification, *Environmental Science and Pollution Research*, 24, pp. 21323-21333.
16. Kiskira, K., Papirio, S., Fourdrin, C., van Hullebusch, E.D. and Esposito, G., (2018). Effect of Cu, Ni and Zn on Fe (II)-driven autotrophic denitrification, *Journal of Environmental Management*, 218, pp. 209-219.

17. Kiskira, K., Papirio, S., Mascolo, M.C., Fourdrin, C., Pechaud, Y., van Hullebusch, E.D. and Esposito, G., (2019). Mineral characterization of the biogenic Fe (III)(hydr) oxides produced during Fe (II)-driven denitrification with Cu, Ni and Zn, *Science of the Total Environment*, 687, pp. 401-412.
18. Kostrytsia, A., Papirio, S., Morrison, L., Ijaz, U.Z., Collins, G., Lens, P.N. and Esposito, G., (2018). Biokinetics of microbial consortia using biogenic sulfur as a novel electron donor for sustainable denitrification, *Bioresource Technology*, 270, pp. 359-367.
19. Li, B., Tian, C., Zhang, D. and Pan, X., (2014). Anaerobic nitrate-dependent iron(II) oxidation by a novel autotrophic bacterium, *Citrobacter freundii* Strain PXL1, *Geomicrobiology Journal*, 31, pp. 138-144.
20. Liu, H., Chen, Z., Guan, Y. and Xu, S., (2018a). Role and application of iron in water treatment for nitrogen removal: a review, *Chemosphere*, 204, pp. 51-62.
21. Liu, Y., Feng, C., Sheng, Y., Dong, S., Chen, N. and Hao, C., (2018b). Effect of Fe (II) on reactivity of heterotrophic denitrifiers in the remediation of nitrate-and Fe (II)-contaminated groundwater, *Ecotoxicology and Environmental Safety*, 166, pp. 437-445.
22. Papirio, S., Ylinen, A., Zou, G., Peltola, M., Esposito, G. and Puhakka, J. A., (2014). Fluidized-bed denitrification for mine waters. Part I: low pH and temperature operation, *Biodegradation*, 25, pp. 425-435.
23. Peng, C., Sundman, A., Bryce, C., Catrouillet, C., Borch, T. and Kappler, A., (2018). Oxidation of Fe (II)–organic matter complexes in the presence of the mixotrophic nitrate-reducing Fe (II)-oxidizing bacterium *Acidovorax* sp. BoFeN1, *Environmental Science & Technology*, 52, pp. 5753-5763.
24. Schaedler, F., Lockwood, C., Lueder, U., Glombitza, C., Kappler, A. and Schmidt, C., 2018. Microbially mediated coupling of Fe and N cycles by nitrate-reducing Fe (II)-oxidizing bacteria in littoral freshwater sediments, *Applied and Environmental Microbiology*, 84, pp. 02013-02017.

25. Shelobolina, E., VanPraagh, C.G. and Lovley, D.R. (2003). Use of ferric and ferrous iron containing minerals for respiration by *Desulfitobacterium frappieri*, *Geomicrobiology Journal*, 20, pp. 143-156.
26. Sorensen, J., (1987). Nitrate reduction in marine sediment: pathways and interactions with iron and sulfur cycling, *Geomicrobiology Journal*, 5, pp. 401–421.
27. Straub, K.L., Benz, M., Schink, B. and Widdel, F., (1996). Anaerobic, nitrate-dependent microbial oxidation of ferrous iron, *Applied and Environmental Microbiology*, 62, pp. 1458-1460.
28. Su, J.F., Ce, C. & Li, W., (2018a). Assessment of Nitrate Removal Coupled with Fe (II) Oxidation and Analysis of Microbial Communities in a Moving-Bed Biofilm Reactor, *Geomicrobiology Journal*, 35, pp. 277-283.
29. Su, J.F., Guo, D.X., Huang, T.L., Lu, J.S., Bai, X.C. and Hu, X.F., (2018b). Sodium carboxymethyl cellulose-modified zero-valent iron used for reduction of nitrate in autotrophic denitrification systems, *Environmental Engineering Science*, 35, pp. 1228-1234.
30. Tian, T., Zhou, K., Xuan, L., Zhang, J.X., Li, Y.S., Liu, D.F. and Yu, H.Q., (2020). Exclusive microbially driven autotrophic iron-dependent denitrification in a reactor inoculated with activated sludge, *Water Research*, 170, pp. 115300-115312.
31. Wang, R., Yang, C., Zhang, M., Xu, S.Y., Dai, C.L., Liang, L.Y., Zhao, H.P. and Zheng, P., (2017). Chemoautotrophic denitrification based on ferrous iron oxidation: reactor performance and sludge characteristics, *Chemical Engineering Journal*, 313, pp. 693-701.
32. Wang, H., Liang, D., Wang, Y.N., Sun, Y., Li, W., Zhang, D., Tsang, Y.F. and Pan, X., (2019). Fabricating biogenic Fe (III) flocs from municipal sewage sludge using NAFO processes: Characterization and arsenic removal ability, *Journal of Environmental Management*, 231, pp. 268-274.
33. Wang, R., Xu, S.Y., Zhang, M., Ghulam, A., Dai, C.L. and Zheng, P., (2020a). Iron as electron donor for denitrification: The efficiency, toxicity and mechanism, *Ecotoxicology and Environmental Safety*, 194, pp. 110343-110352.

34. Wang, Y., Lin, Z., Huang, W., He, S. and Zhou, J., (2020b). Electron storage and resupply modes during sulfur cycle enhanced nitrogen removal stability in electrochemically assisted constructed wetlands under low temperature, *Bioresource Technology*, 300, pp. 122704-122715.
35. World Health Organisation (WHO) and World Health Organisation Staff, (2004). Guidelines for drinking-water quality (Vol. 1). World Health Organization.
36. Zhang, M., Zheng, P., Li, W., Wang, R., Ding, S. and Abbas, G. (2015). Performance of nitrate-dependent anaerobic ferrous oxidizing (NAFO) process: a novel prospective technology for autotrophic denitrification, *Bioresource Technology*, 179, pp. 543-548.
37. Zhang, M., Zhangzhu, G., Wen, S., Lu, H., Wang, R., Li, W., Ding, S., Ghulam, A. and Zheng, P., (2018). Chemolithotrophic denitrification by nitrate-dependent anaerobic iron oxidizing (NAIO) process: Insights into the evaluation of seeding sludge, *Chemical Engineering Journal*, 345, pp. 345-352.
38. Zhang, Y., Douglas, G.B., Kaksonen, A.H., Cui, L. and Ye, Z., (2019). Microbial reduction of nitrate in the presence of zero-valent iron, *Science of the Total Environment*, 646, pp.1195-1203.
39. Zhou, J., Wang, H., Yang, K., Ji, B., Chen, D., Zhang, H., Sun, Y. and Tian, J., (2016). Autotrophic denitrification by nitrate-dependent Fe (II) oxidation in a continuous up-flow biofilter, *Bioprocess and Biosystems Engineering*, 39, pp.277-284.
40. Zou, G., Papirio, S., Ylinen, A., Di Capua, F., Lakaniemi, A. M. and Puhakka, J. A., (2014). Fluidized-bed denitrification for mine waters. Part II: effects of Ni and Co, *Biodegradation*, 25, pp. 417-423.
41. Zou, G., Papirio, S., van Hullebusch, E. D. and Puhakka, J. A., (2015). Fluidized-bed denitrification of mining water tolerates high nickel concentrations, *Bioresource Technology*, 179, pp. 284-290.